Supplementary Information (SI) for Analyst.
This journal is © The Royal Society of Chemistry 2026

Supporting Information

Digital Microfluidic Integrated SiNW Arrays FET for Amplification-Free Detection of Extracellular Vesicle -derived miRNA

Rui Jiang[1,2], Jiaqi Guo[1,2], Zizhen Wang[1,2], Jun Cheng[1,2], Han Zhang[1,2], Qingzhu Zhang[1], Lingqian Zhang[1], Yang Zhao[1], Chengjun Huang[1,2], Mingxiao Li[1,*]

[1]Institute of Microelectronics of the Chinese Academy of Sciences, Beijing 100029, China

[2]University of Chinese Academy of Sciences, Beijing 101408, China

* Corresponding author.

E-mail addresses: limingxiao@ime.ac.cn

Note S1. Dual-antibody functionalization on magnetic beads

Dual antibody-modified magnetic beads were prepared using 1μm magnetic beads from Dongna Biotechnology. In short, after washing and resuspending the magnetic beads in MES solution, the carboxylic acid groups on the beads were activated using 10 mg/mL (w/v) EDC solution and sulfo-NHS solution. 200 μL of activated magnetic beads were incubated with 20 μL of dual antibodies: 15 μL of CD63 antibody at a concentration of 100 μg/mL (v/v), and 5 μL and 10 μL of CD9 antibody at a concentration of 100 μg/mL (v/v), respectively, at 37°C for 1 h in a shaker. Following subsequent experiments, the magnetic beads were blocked with 1% BSA (v/v) at 37°C in a shaker for 1 h, washed three times with PBS (1 × PBS, pH = 7.4), and then resuspended in 100 μL PBS[1]. The prepared magnetic beads were used for EV enrichment and characterization on the DropFET Device magnetic control module.

Note S2. Methods for EV characterization.

Isolation of extracellular vesicles. Extracellular vesicle (EV) samples were extracted from cell culture supernatant using ultracentrifugation. All centrifugation was performed at 4 °C to minimize EV structural damage and protein degradation. The specific procedure was as follows: First, the supernatant was centrifuged sequentially at 300 g for 10 min to remove residual cells. Then, it was centrifuged at 2000 g for 20 min to remove cell debris, and finally at 10000 g for 30 min to remove large vesicles and biomolecules. Next, the resulting supernatant was ultracentrifuged at 110000 g for 70 min, and the EVs were collected and resuspended in pre-chilled 1×PBS. Finally, it was ultracentrifuged again at 110000 g for 70 min to remove soluble protein contaminants, the supernatant was discarded, and the final EV precipitate was resuspended in ≤200 μL PBS. A portion of the separated EVs was used for structural and particle size characterization, while the remaining samples were stored at -80 ℃.

Transmission electronic microscopy (TEM). For TEM characterization, the exosome sample was diluted to 1 mg/mL and fixed overnight at -4 ℃ with 2.5% glutaraldehyde. Then, 10 μL of the fixed exosome sample was added onto a copper grid that had been plasma-cleaned. After standing for 10 minutes, the excess sample was aspirated, and then 10 μL of uranium acetate staining solution was added for negative staining. After standing for 1 min, the excess staining solution was aspirated, and after natural drying, the morphology was observed using TEM[2].

Western blotting (WB). First, the extracted exosome samples were mixed with RIPA lysis buffer and lysed on ice for 30 minutes, followed by centrifugation at 12000 g and 4 °C for 10 min. The supernatant of the total protein sample was collected. Protein concentration was determined using a BCA protein quantification kit, and equal volumes of protein were separated by SDS-PAGE electrophoresis. The protein was transferred to a PVDF membrane and blocked in 5% skim milk at room temperature for 1 h. Primary antibodies against CD9, CD63, and TSG101 were added, and the membrane was incubated overnight at 4 °C. The membrane surface was washed three times with TBST, and then HRP-labeled secondary antibodies were added and incubated at room temperature for 1 h. Finally, chemiluminescence (ECL) was used for color development, and band signals were acquired using an imaging system to analyze the expression of exosome membrane proteins.

Nanoparticle tracking analysis (NTA). The particle size distribution and concentration of EVs were determined using a nanoflow cytometer (U30E, Xiamen Fuliu). Instrument QC calibration was performed by diluting 3 μL of quality control (QC) beads 10-fold with ultrapure water, followed by a further 10-fold dilution of 10 μL of the mixture. Exosome samples were serially diluted 10-fold, 100-fold, and 1000-fold to reach the counting range. After removing the PBS blank control and applying a low threshold to remove background signals, the particle size distribution and concentration were determined.

Note S3. Methods for EVs-miRNA qRT-PCR assays.

Total RNA was extracted from lysed EVs using a commercially available total RNA extraction kit, following the kit instructions. For cDNA synthesis, approximately 2 μg of total RNA was reverse transcribed into cDNA using SuperScript III reverse transcriptase (Invitrogen), with a final reaction volume of 20 μL. The reverse transcription program was: 42 °C for 60 min, followed by heating at 95 °C for 3 mins to inactivate the enzyme. The obtained RT product was diluted 10-fold with nuclease-free water and used as a template for subsequent qPCR analysis[2,3].

Quantitative real-time PCR was performed using miRNA SYBR & ROX premix. The total reaction volume was 20 μL, containing 10 μL of 2 × miRNA premix, 2 μL of diluted RT product, 0.4 μL of forward primer, 0.4 μL of reverse primer, and made up to the nearest whole number with nuclease-free water. To ensure accuracy and reproducibility of pipetting, two additional reactions were performed. The premix was prepared on ice and then aliquoted into each well of a 96-well plate before adding the template. PCR amplification was performed on a real-time quantitative PCR instrument under the following conditions: initial denaturation at 95 °C for 15 min, followed by 40 cycles, each cycle consisting of denaturation at 94 °C for 20 s and annealing/extension at 60 °C for 34 s. Melting curve analysis was performed after amplification to verify specificity.

Table S1 Sequences and involved probes[4,5]

Probe name	Sequences（5' - 3'）
miRNA-21	UAGCUUAUCAGACUGAUGUUGA
miRNA-155	UUAAUGCUAAUCGUGAUAGGGGU
M1	UAGCUUAUCACACUGAUGUUGA
M2	UAGCUUAUAAGACUAAUGUUGA
M3	UUGCUUAUCGGACUGAUCUUGA
M4	UAAACCAUCCCACUCGGCGGCA
miRNA-10b	UACCCUGUAGAACCGAAUUUGUG
Probe-155	5' - NH2 C6-ACCCCUAUCACGAUUAGCAUUAA - 3'
Probe-21	5' - NH2 C6-TCAACATCAGTCTGATAAGCTA - 3'
hsa-miR-155 Forward Primer	TTAATGCTAATCGTGATAGGGGTT
hsa-miR-155 Reverse Primer	CAGTGCGTGTCGTGGAGT
hsa-miR-21 Forward Primer	TAGCTTATCAGACTGATGTTGA
hsa-miR-21 Reverse Primer	CAGTGCGTGTCGTGGAGT

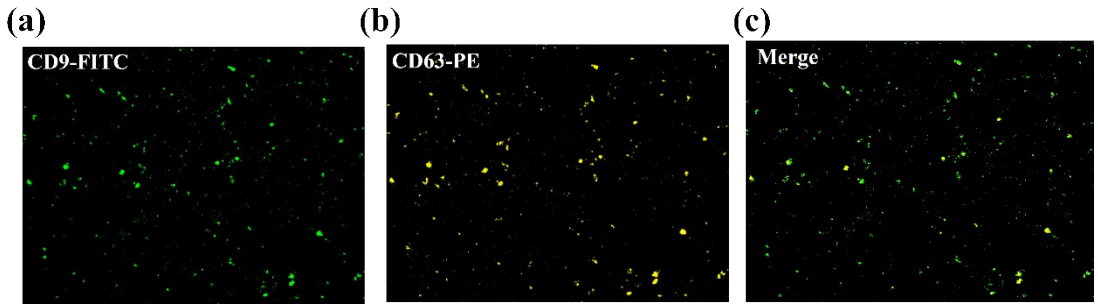

Figure. S1 Fluorescence characterization of dual antibody-modified magnetic beads. (a) Magnetic beads modified with FITC-labeled CD9 antibody, (b) Magnetic beads modified with PE-labeled CD63 antibody, and (c) Fluorescence image of merged.

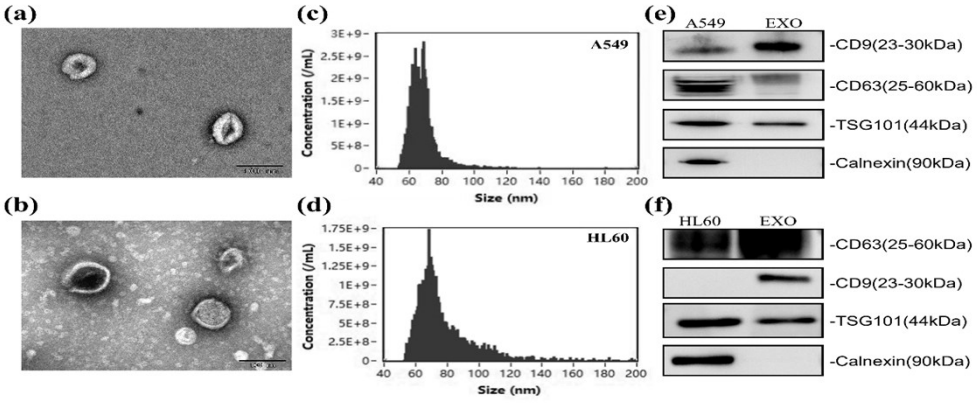

Figure. S2 Characterization of EVs. (a) TEM image of A549-derived EVs. (b) TEM image of HL60-derived EVs. (c) NTA analysis of the size distribution of EVs derived from A549 cells. (d) NTA analysis of the size distribution of EVs derived from HL60 cells. (e) Western blotting displays the expression of protein markers (CD63, CD9, TSG101, and Calnexin) in A549-derived EVs. (f) Western blotting displays the expression of protein markers (CD63, CD9, TSG101, and Calnexin) in HL60-derived EVs.

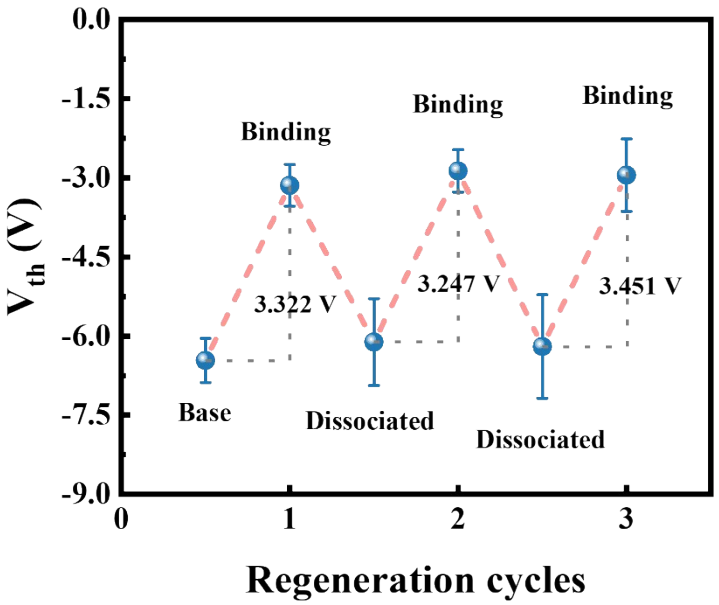

Figure. S3 Reusability of the DropFET. Error bars represent standard deviations (n = 3).

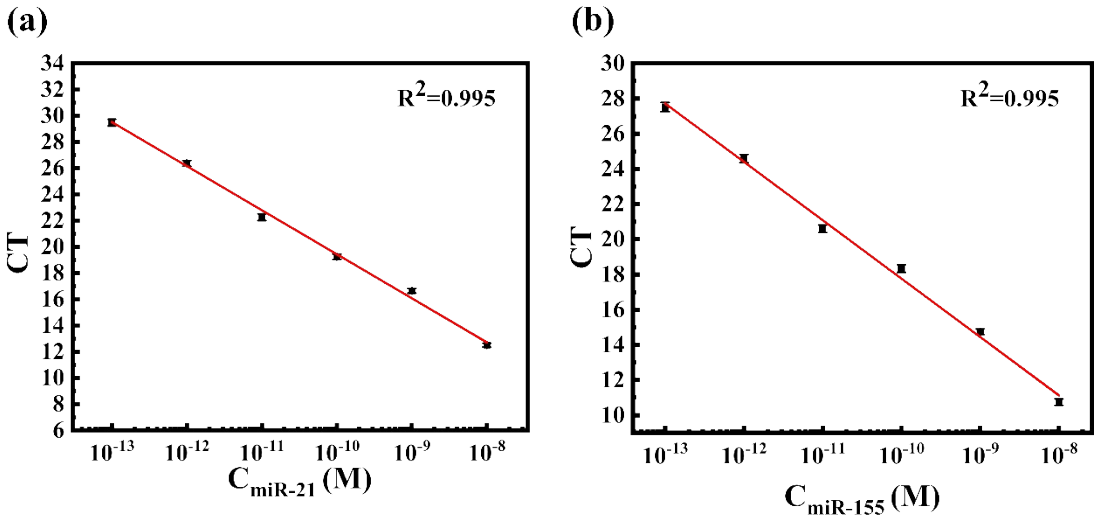

Figure. S4 Standard curves of miRNA-21(a) and miRNA-155(b) concentrations determined by qRT-PCR.

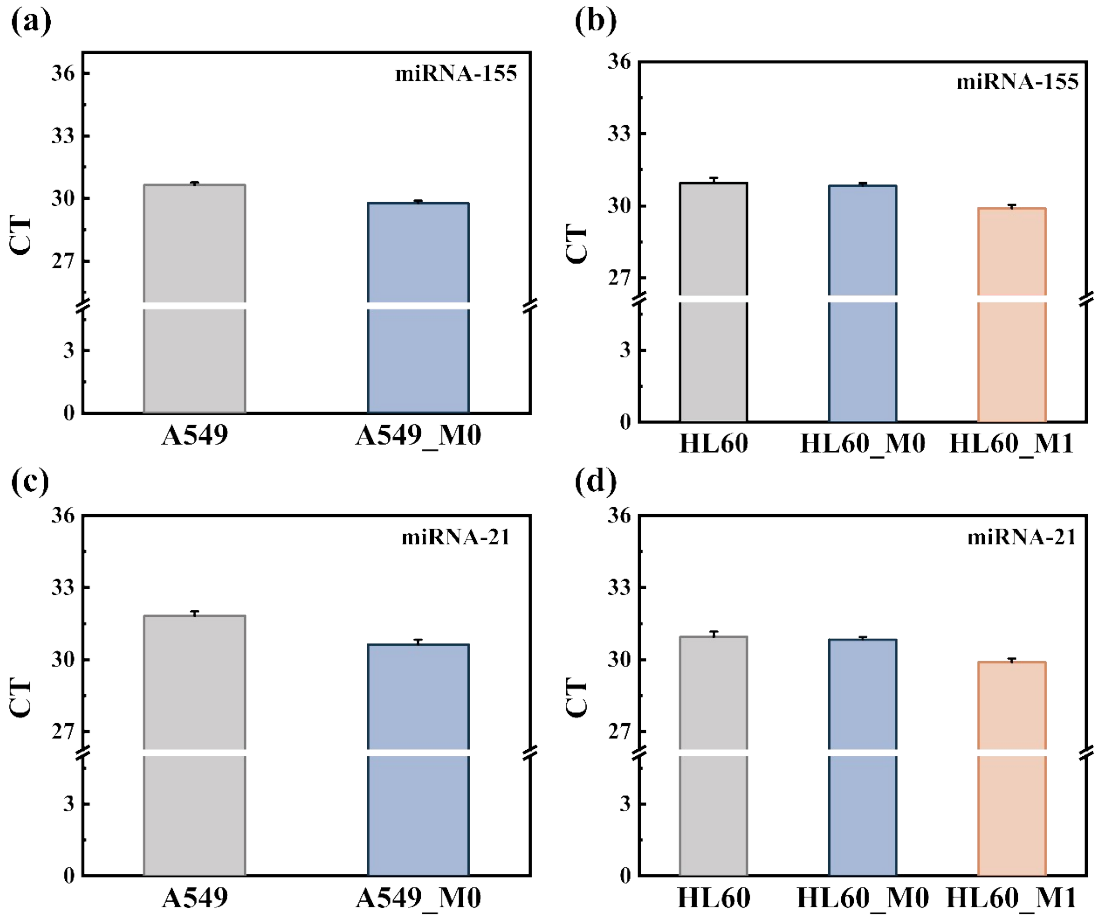

Figure. S5 qRT-PCR results of exosomal miRNA-21 and miRNA-155. (a) CT values of miRNA-155 in A549 EVs of normal cells and acute lung injury model. (b) CT values of miRNA-155 in HL60 EVs under normal, induced differentiation, and inflammatory models. (c) CT values of miRNA-21 in A549 EVs of normal cells and acute lung injury model. (d) CT values of miRNA-21 in HL60 EVs under normal, induced differentiation, and inflammatory models.

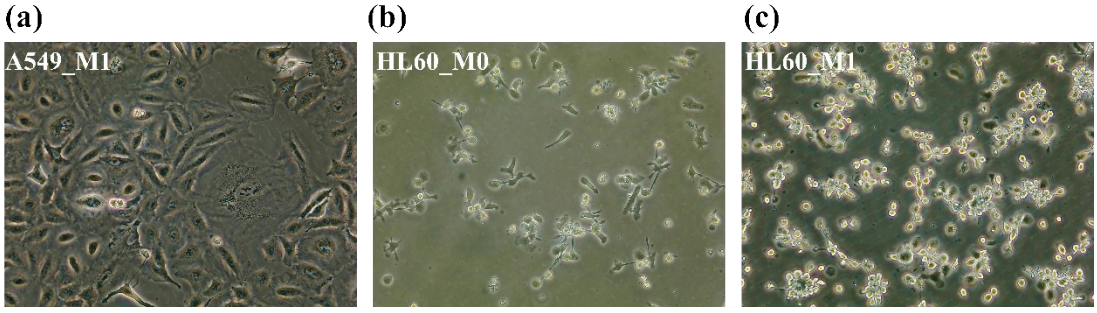

Figure. S6 Cell states and bioactivity during the induction of differentiation and inflammation model of two cell lines. (a) A549 cells (A549_M1) after the construction of the acute lung injury model. (b) HL60 cells (HL60_M0) after induction of differentiation. (c) HL60 cells (HL60_M1) after the construction of the inflammation model.

References

1 C. Wang, D. Jin, Y. Yu, L. Tang, Y. Sun, Z. Sun and G.-J. Zhang, *Sensors and Actuators B: Chemical*, 2020, **314**, 128056.
2 Z. Tong, X. Xu, C. Shen, D. Yang, Y. Li, Q. Li, W. Yang, F. Xu, Z. Wu, L. Zhou, C. Zhan and H. Mao, *Biosensors and Bioelectronics*, 2025, **270**, 116976.
3 Y. Li, Y. Dou, Z. Lu, Y. Wang, H. Zhou and T. Li, *Biosensors and Bioelectronics*, 2025, **289**, 117936.
4 N. H. H. Heegaard, A. J. Schetter, J. A. Welsh, M. Yoneda, E. D. Bowman and C. C. Harris, International Journal of Cancer. 2012, **130**,1378-1386.
5 Y. Xing, *Chem. Eng. J.*, 2024, **488**, 150987.